PERFORMANCE OF CHANNEL CODING ON FREE SPACE OPTICAL (FSO) COMMUNICATION LINK

AMMAR ABOTABEK

AUGUST 2014

PERFORMANCE OF CHANNEL CODING ON FREE SPACE OPTICAL (FSO) COMMUNICATION LINK

A THESIS SUBMITTED TO

THE GRADUATE SCHOOL OF NATURAL AND APPLIED SCIENCES
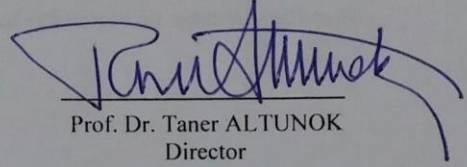
OF

ÇANKAYA UNIVERSITY

BY

AMMAR ABOTABEK

IN PARTIAL FULFILLMENT OF THE REQUIREMENTS

FOR

THE DEGREE OF MASTER OF SCIENCE

IN

THE DEPARTMENT OF

ELECTRONIC AND COMMUNICATION ENGINEERING

AUGUST 2014

Title of the Thesis: **Performance of Channel Coding on Free Space Optical (FSO) Communication Link**
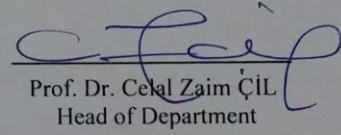
Submitted by **Ammar ABOTABEK**

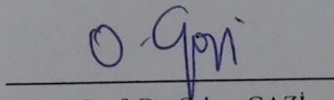Approval of the Graduate School of Natural and Applied Sciences, Çankaya University.

Prof. Dr. Taner ALTUNOK
Director

I certify that this thesis satisfies all the requirements as a thesis for the degree of Master of Science.
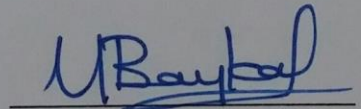
Prof. Dr. Celal Zaim ÇİL
Head of Department

This is to certify that we have read this thesis and that in our opinion it is fully adequate, in scope and quality, as a thesis for the degree of Master of Science.

Assoc. Prof. Dr. Orhan GAZİ
Co-supervisor

Prof. Dr. Yahya Kemal BAYKAL
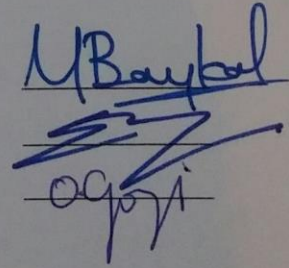Supervisor

Examination Date: 18.08.2014

Examining Committee Members

Prof. Dr. Yahya Kemal BAYKAL   (Çankaya Univ.)

Prof. Dr. Erdem YAZGAN   (Hacettepe Univ.)

Assoc. Prof. Dr. Orhan GAZİ   (Çankaya Univ.)

STATEMENT OF NON-PLAGIARISM PAGE
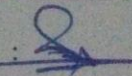
I hereby declare that all information in this document has been obtained and presented in accordance with academic rules and ethical conduct. I also declare that, as required by these rules and conduct, I have fully cited and referenced all material and results that are not original to this work.

Name, Last Name : Ammar ABOTABEK

Signature   :

Date   : 18.08.2014

ABSTRACT

PERFORMANCE OF CHANNEL CODING ON FREE SPACE OPTICAL (FSO) COMMUNICATION LINK

ABOTABEK, Ammar

M.Sc., Department of Electronic and Communication Engineering

Supervisor: Prof. Dr. Yahya Kemal BAYKAL

Co-supervisor: Assoc. Prof. Dr. Orhan GAZİ

August 2014, 33 pages

The average loss power and the channel fading are among the major challenges of the free-space optical (FSO) communications through the turbulent atmosphere, resulting in the bit-error-rate (BER) performance degradation, or even communication link outage. For the same average received optical signal power, the degradation in BER performance is strongly dependent on the fading statistics. This thesis investigates the performance of channel coding to improve the FSO communication system performance and the communication distance by mitigating atmospheric turbulence. We derive a pairwise error probability (PEP) expression considering the recently introduced gamma-gamma turbulence model and then we drive the upper bounds for the bit-error probability for block codes through atmospheric turbulence channels, considering the gamma-gamma model. Also we present numerical results for the BER

performance of different codes such as the Reed-Solomon (RS), Bose, Chaudhuri, and Hocquenghem (BCH) and Hamming codes under different turbulence conditions (weak, moderate, strong).

ÖZ

SERBEST UZAY OPTİK (FSO) HABERLEŞME LİNKİ ÜZERİNDE KANAL KODLAMA PERFORMANSI

ABOTABEK, Ammar

Yüksek Lisans, Elektronik ve Haberleşme Mühendisliği Anabilim Dalı

Tez Yöneticisi: Prof. Dr. Yahya Kemal BAYKAL

Eş- Tez Yöneticisi: Doç. Dr. Orhan GAZİ

Ağustos 2014, 33 sayfa

Ortalama güç kaybı ve kanal sönümlemesi, türbülanslı atmosferden dolayı bit hata oranı (BER) performansının bozulması, hatta haberleşme link kesintisine neden olması, serbest uzay optik (FSO) haberleşmelerinin başlıca zorlukları arasında yer almaktadır. Aynı ortalama optik sinyal gücü için, BER performansındaki bozulma sönümleme istatistiklerine bağlıdır. Bu tez, atmosferik türbülansı azaltarak FSO haberleşme sistemi performansını ve haberleşme mesafesini geliştirmek için kanal kodlamasının performansını incelemektedir. Yakın zamanda tanıtılmış gamma-gamma türbülans modelini değerlendiren ikili hata olasılığı (PEP) ifadesinden yola çıkarak ve sonrasında gamma-gamma modelini ele alarak, atmosferik türbülans kanalları aracılığıyla blok kodları için üst sınır bit-hata olasılığı kullanılmıştır. Aynı

zamanda, Reed- Solomon (RS), Bose, Chaudhuri, and Hocquenghem (BCH) ve Hamming gibi farklı kodlar ve farklı türbülans koşulları (zayıf, orta, güçlü) için bit hata oranı performansının sayısal sonuçları sunulmuştur.

Anahtar kelimeler: FSO Haberleşmesi, Kanal Kodlaması, Atmosferik Türbülans Kanalı, PEP.

ACKNOWLEDGEMENT

TABLE OF CONTENTS

LIST OF FIGURES

FIGURES

LIST OF ABBREVIATIONS

FSO	Free Space Optical
RF	Radio Frequency
BER	Bit Error Rate
PDF	Probability Density Function
OOK	On Off Keying
BCH	Bose, Chaudhuri, and Hocquenghem
IM/DD	Intensity Modulated/ Direct Detection
PEP	Pairwise Error Probability
RS	Reed-Solomon Code
LED	Light Emitting Diode
LD	Laser Diode
AWGN	Additive White Gaussian Noise
CSI	Channel State Information
MDS	Maximum Distance Separable
SNR	Signal to Noise Ratio
MIMO	Multiple-Input Multiple-Output

CHAPTER 1

INTRODUCTION

1.1. Motivation

A Free Space Optical (FSO) communication system is a form of Optical Communication Technology, it is able to wirelessly function (using propagating light in free-space) in order to transmit data for computer networking or telecommunications.

FSO is known for its variety of uses that are associated with a wide range of applications, these include for example safety addons for vital fibre networks, space communications, temporary network installations, the last-mile solutions, LAN-to-LAN connections, aircraft-to-aircraft communication and military applications [1–6]. There are many advantages to the FSO communication systems when compared to fibre optics and other wireless communication systems such as radio frequency (RF), these are:

- Greater bandwidth
- Advanced antenna gain
- Improved privacy
- Slighter antenna component sizes
- No digging
- Mobility possible
- The lasers used are eye safe
- Easy to install,
- Set up a link in a short time

1

- No interference
- Immunity to interference between links operating in different rooms
- High security
- Inexpensive component
- License-free operation [7-8].

However, there are many challenges associated with free space optical communications, this involves the light that propagates through the free-space of the unsettled atmosphere, because when this occurs it causes the wandering of the laser beam and eventually it will face refractive indexes that will randomly fluctuate along its path. These fluctuations will cause the beam to broaden and scintillation, will also result in unplanned distortions in the wave-front and the stern line-of-sight is required to have exact directing and occasionally a receiver at the tracking mechanisms [9–16].

There is an optical link to the weather conditions that is known to be susceptible making it a highly important issue to be considered, especially the effects of aerosol scattering that occurs as a result of all the seasons involving rain, fog, sand storm and snow. These effects can cause a reduction in the range of linkage that is associated with the loss of propagation in a non-clear atmosphere. In clear atmospheric conditions, variations can be found along the transmission pathway of the air refractive index because of the occurrence of solar heat and wind from the pressure and temperature of inhomogeneities.

Both power loss that is received averagely (known as channel fading at the receiver aperture) and power fluctuation that is received instantaneously are a result of all these effects. Bit Error Rate (BER) system is increased with a decrease in reliability and channel capacity are caused by power loss incorporation with fading. In addition to this, intense communication outages may occur from deep power fades.

There are many solutions to power loss and moderate fading issues, one of these solutions is dependent on the optical propagation domain by developing the FSO communication channel. These are achieved by employing, for example, adaptive

optics, multiple aperture receiver, larger receiver aperture sizes and multiple aperture transmitter [17–19].

A beam that is diverged slightly may be possibly used to decrease the deep fades for beam wander induced optical power fading, though a disadvantage of using a diverged beam is that it will consequence in a loss of the average received power significantly. If the coherent radius is smaller than the diameter of the receiver aperture then the fading level is reduced, since a larger aperture decreases the level of fading. This process of optical scintillation is defined as aperture averaging, hence it is a vital reason out of many when handling receiver apertures of large sizes for the application of direct detection systems. Generally, larger receiver apertures have the ability of collecting more optical signals with the reduction of channel fading, in addition to this further background noise is collected. For that reason, the use of a receiver aperture of a large size that is greater than or approximate to the size of the long term laser spot is beneficial, because the loss of performance as a result of increased noise may not be balanced.

A further solution is the application of channel coding for the achievement of reliable and effective communication through the FSO fading channel. The channel capacity is a number that is associated with every communication channel, its properties include having the highest rate for transmitting information that can be achieved through the channel with reliable communication. The channel coding is a necessary aspect in order to approach the capacity of the channel ensured by the information theory, also for the achievement of reliable information transmission for systems of modern communication [20–22]. The improvement of the error rate performance can be accomplished by the use of diversity techniques in corporation to error control coding over FSO links.

The simplicity of the Log-normal distribution model allows it to be used for the probability density function (PDF) of the irradiance, hence it is the most widely used model for this purpose although it only applies to weak turbulence conditions [11]. Numerous scattering effects are to be considered with the increasing strength of turbulence, where in some cases log-normal statistics can be found to display large

3

deviations when compared to experimental data. In addition, log-normal PDF has shown to underestimate the behaviour of the tails in comparison to the results of the measurement. The probabilities of fading and detection are based on the foundation of the tails of the pdf, if this area is underestimated then the accuracy of the performance analysis is affected significantly as a result. A variety of turbulence conditions can be associated with the description of atmospheric turbulence channels, these have been suggested over the years as statistical models along with many others because of the limits that the log-normal model proposes. The log-normal channel, the I-K distribution and the K distribution are the turbulence conditions that are involved [4]. Several researchers are known to use the gamma-gamma pdf for the modelling of atmospheric turbulence as a manageable mathematical model [23-26]. The gamma-gamma pdf model has suitability that designates both turbulence regimes, strong and weak. This is a model with a two parameter distribution that is dependent on a doubly stochastic theory of scintillation, while assuming that fluctuations of large-scale irradiance control fluctuations of small-scale irradiance of the propagating wave, since both of these are directed by independent gamma distributions. The gamma-gamma pdf is directly linked to the conditions associated with the atmosphere proving a well fitting for experimental data.

In this thesis, we consider the gamma-gamma pdf model and the (OOK) on-off keying modulation, assuming that the receiver and transmitter alignment is perfect and without the consideration of other effects for example the building sway. Furthermore, the atmospheric loss that is related to the visibility is neglected, focusing on the mitigation of the channel fading ascending from the scintillation. We study three kind of codes, Reed-Solomon, Hamming and BCH codes.

1.2. Previous Work

Diversity technique in addition to error control coding are applied for the improvement of the performance of the error rate. Error control coding has the ability to assist in mitigating turbulence induced signal fading in the FSO communication system through atmospheric turbulence. In [18], [27], the coded FSO links performance is studied by the assumption of a log-normal channel model for the atmospheric

turbulence. This is specific to an approximate upper bound that is resultant for the PEP for the coded FSO links with the intensity modulation/direct direction (IM/DD), this provides the bit error rate (BER) with upper bounds on it with the use of the transfer function technique. In [23]-[25], attention is focused on the gamma-gamma pdf distribution for its exceptional fit with the measurement data of turbulence conditions of a wide range of weak to strong. In [28], an investigation into the error performance of coded FSO links by the assumption that OOK is controlled by the fading process with gamma-gamma pdf distribution, convolutional encoding, Viterbi decoding and the channel distortion by the addictive white Gaussian noise. An estimated PEP is resultant for the coded FSO links with IM/DD. In this paper [28], a description can be found on the obtainment of BER performance with the application of the transfer function technique together with the resultant PEP expression.

In this thesis, we investigate the error performance of coded FSO links with the assumption of OOK modulation and gamma-gamma pdf model. We derived an approximate PEP for the coded FSO links and obtained the BER performance for block codes (Reed-Solomon, Hamming and BCH codes) by using the transfer function technique.

1.3. Aim of Thesis

The aim of this thesis is to evaluate the performance of channel coding in an FSO communication system experiencing atmospheric turbulence. Three very popular channel codings are to be considered for the aspect of this purpose that are regularly active in optical communication systems: Reed-Solomon (RS) codes, Hamming codes, and BCH code. We reflect on a realistic statistical channel model that has lately been suggested for the optical wireless systems, including the gamma-gamma model. A comparison will be undergone on the performance of the system depending on the average BER for the various coding schemes and various turbulence conditions.

1.4. Thesis Outline

The organization of the thesis is as follows:

- **In Chapter 1**, The Introduction, Motivation, Previous Work and the Aim of thesis is provided.

- **In Chapter 2,** Background review and channel characteristics are presented.

- **In Chapter 3**, PEP derivation for FSO communication systems with OOK are presented.

- **In Chapter 4**, The derivation of the upper bounds on the bit-error probability of the codes are presented and a brief analysis of the three channel coding techniques that are considered in this thesis (RS, BCH and Hamming) are given

- **In Chapter 5**, Numerical results and BER performance to compare the performances of the suggested coding schemes under various codes and different turbulence conditions are presented.

- **In Chapter 6**, Conclusion and future work are given.

CHAPTER 2

BACKGROUND REVIEW

FSO communication system is the transmission and the reception of information through free space medium. There are three basic components that comprise all communication systems which are the receiver, the channel and the transmitter. The transmitter is comprised of an encoder and a modulator. Its function is to encode the information bits, often with an error-correction code, and convey that information with an optical wave. FSO systems are capable of transmitting several gigabits of information per second along line of sight paths through the turbulent atmosphere. Other attractive attributes of FSO communication systems include lower mass, power, and volume compared with conventional radio frequency (RF) systems, and a narrow-beam with high gain, which means a more secure channel.

2.1. Optoelectronic Components

FSO communication system component contains light emitting devices such as lasers and light emitting diode (LED) in the transmitter and photodetectors in the receiver.

2.1.1. In the Transmitter

They are two kinds of light emitting devices, these are light emitting diodes and laser diodes. A laser diode (LD) is a semi-conductor that is electrically pumped, the active medium is produced by a p-n junction of the semiconductor diode. An LD is a more modern form of technology which has developed from underlying LED fabrication techniques. LED is a two lead semi-conductor light source that is similar to a simple pn-junction diode, hence when activated this property enables it to emit light. The speed of operation between LED and LD is the key advantage of LD over LED. The

modulation bandwidth of LD is up to tens of GHz and for LED the modulation bandwidth is up to hundreds of MHz but the LD must be rendered eye safe, and is more expensive than LED.

2.1.2. In the Receiver

Solid-state devices that undergo the inverse operation of the light emitting devices are called photodetectors and may also be known as photodiodes. They have the ability to convert electrical current from incident radiant light. There are two kinds of photodetectors, p-i-n photodiode and avalanche photodiode. Avalanche photodiode is a popular and widely used detector because of its small portable size, relatively low cost, good responsivity and high accuracy. A p-i-n photodiode works by mostly generating one electron-hole pair per photon while avalanche photodiodes function by providing a gain that is associated with the generated photocurrent. The modulation bandwidth of avalanche photodiode is from hundreds of MHz up to tens of GHz, and for p-i-n photodiode it is from tens of MHz up to tens of GHz. Also p-i-n photodiode is lower cost when compared with the avalanche photodiode [29].

2.2. Free Space Optical Channel Topologies:

There are three popular FSO channel topologies:

2.2.1. Point-to-Point Links

When there is an unobstructed hence direct path between a receiver and transmitter then the point-to-point FSO link is operated. The link is recognised when the transmitter is leaning towards the receiver. The point-to-point topology is known as low complexity, this means that in order for it to accomplish high data rate links there are pointing requirements and the expense of mobility. Therefore, pointing is an essential requirement of this link topology, and also it has blocking and shadowing sensitivity, these are the main limitation associated with this link topology. Point-to-point wireless optical links have been employed in an extensive variety of long-range and short-range applications. Point-to-point link can be employed in the long range

outdoor optical link, where a multi-gigabit per second transmission is possible over 4km [29]. There has been a consideration of ultra-long range point-to-point links for earth-to-space communications.

2.2.2. Diffuse Links

Pointing and shadowing problems of point-to-point links can be eased by diffuse transmitters that radiate optical power above a varied solid angle. The radiant optical power is presumed to reflect from the room surfaces, therefore the transmitter is not required to be pointed at the receiver. This makes it affordable for user terminals to have an extensive amount of mobility at the cost of a path loss that is high [29]. Diffuse links encounter a high path loss however they provide a large level of robustness and mobility.

2.2.3. Quasi-Diffuse Links

Quasi-diffuse links are made up of features of both diffuse links and point-to-point links. The transmitter lightens up the ceiling with a sequence of beam sources diverging slowly, this illumination on the ceiling creates a grid of spots [29]. They are responsible for higher data rates by making it necessary for users to point their receivers to the ceiling, although this causes the encountering of greater implantation cost as a result of the multi-beam transmitter.

2.3. Wavelength Choice

A large number of FSO users have been using the 780-850 nm near infrared spectrum because of reasons due to cost. Nonetheless, the fibre-optic telecommunication industry has chosen the 1550nm band, since it is of a higher suitability for optical wireless. Compared to the 780 nm band the 1550 nm band can transmit more power and is safer for human eyes because of the properties of the human eye. Another difference is that the 1550nm band has a power density that is approximately fifty times safer than the 780nm band [30].

2.4. Intensity Modulated Direct Detection (IM/DD) Systems

The most frequently used system in free space optical communication system is the IM/DD. In free space optical systems, the intensity of an optical source is modulated to transmit the signals. The intensity of the light wave is modulated based on the information signal. This technique is simple because the intensity modulation (IM) can be accomplished via the variations of the bias current of an LD or LED. The simplest configuration that can function for the detection of an intensity modulated signal is known as direct detection (DD). A photocurrent is generated by a photodetector in a DD receiver that is proportional to the rapid optical power received. The most well-known scheme used in free space optical communication systems is the OOK scheme [29-30]. An advantage of this scheme is that they usually have inexpensive implementations and simple. We only present a brief review of OOK.

2.4.1. On-Off Keying

OOK is a common modulation scheme in free space optical communication system. Also OOK is the simplest type of binary modulation. In an active high OOK encoding, a "1" is coded as a pulse, while a "0" is coded as no pulse or off field, as shown in Fig. 1.
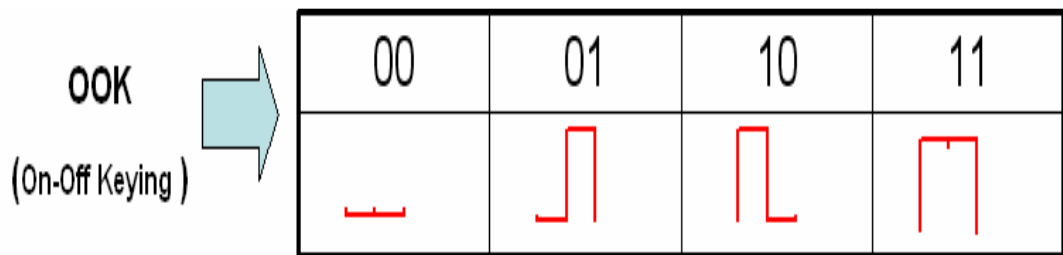

Figure 1: Basic OOK signal

OOK is an appropriate modulation scheme for high bit rate FSO systems [32] due to its simplicity and the ability of LD/LED to switch on and off at rates into Gbit/s.

2.5. Probability Density Function (PDF) System Models

The performance of free optical communication system can be severely degraded by turbulence induced fluctuations in the received signal, known as scintillation. Scintillation can result in the loss of the received power or fading of the signal under a prescribed threshold [30]. The reliability of an FSO system can be deduced from a mathematical model for the pdf of the fluctuating signal [30].

Many pdfs have been suggested as models for the function of distribution for the irradiance fluctuations. Here we present a brief review of two pdf models that are seen as the models with the broadest acceptance in the gamma-gamma pdf, the lognormal pdf and the literature.

2.5.1. Lognormal PDF Model

The lognormal pdf is usually approved as a representative model for irradiance fluctuations in the scintillation regime that is weak. The expression for the lognormal distribution is used in this study, it can be found in [31].

$$P(I) = \frac{1}{I\sqrt{2\pi\sigma_{lnI}^2}}exp\left\{-\frac{\left[\ln(I) + \frac{1}{2}\sigma_{lnI}^2\right]^2}{2\sigma_{lnI}^2}\right\}, \qquad I > 0 \qquad (2.1)$$

where σ_{lnI}^2 is the log-irradiance variance. In the weak scintillation regime the scintillation index σ_I^2 is approximately equal to σ_{lnI}^2, where

$$\sigma_{lnI}^2 = \ln(\sigma_I^2 + 1) \qquad (2.2)$$

2.5.2. Gamma-Gamma PDF Model

The PDF model gamma-gamma appropriately describes weak and strong turbulence regimes [24-26]. In this model, the scintillation that induces the intensity fluctuation

11

is modelled is a process where the small scale (also known as diffractive) intensity fluctuations are multiplicatively controlled by large scale (also known as refractive) fluctuations [24-26]. Let us denote the large- and small-scale irradiance fluctuations by I_x and I_y, in turn. I_x and I_y are expected to be statistically independent and designated by a gamma distribution. Depending on these expectations, the intensity fluctuation $I = I_x I_y$ has a gamma-gamma pdf with the probability density function as follows

$$f(I) = \frac{2(\alpha\beta)^{\frac{(\alpha+\beta)}{2}}}{\Gamma(\alpha)\Gamma(\beta)} I^{\frac{\alpha+\beta}{2}-1} K\alpha - \beta\left(2\sqrt{\alpha\beta I}\right) \tag{2.3}$$

where $K_\alpha(.)$ is the modified Bessel function of the second kind of order a. Here, α and β are the effective number of large scale and small scale eddies of the scattering environment.

$$\alpha = \left[exp\left(\frac{0.49x^2}{\left(1 + 0.18d^2 + 0.56x^{12/5}\right)^{7/6}} \right) - 1 \right]^{-1} \tag{2.4}$$

$$\beta = \left[exp\left(\frac{0.51x^2\left(1 + 0.69x^{12/5}\right)^{-5/6}}{\left(1 + 0.9d^2 + 0.62d^2 x^{12/5}\right)^{5/6}} \right) - 1 \right]^{-1} \tag{2.5}$$

where $x^2 = 0.5 C_n^2 k^{7/6} L^{11/6}$ and $d = \left(\frac{kD^2}{4L}\right)^{1/2}$ Here, $k = \frac{2\pi}{\lambda}$ is the optical wave number, λ is the wavelength, D is the diameter of the receiver that collects the lens aperture and L is the link distance in meters. C_n^2 Represents the index of refraction structure parameter and is altitude-dependent. Numerous C_n^2 profile models are present in the literature, one of which is given as

$$C_n^2 = 0.00594(v/27)^2(10^{-5}h)^{10} exp(h/1000) + 2.7 \times 10^{-6} \exp(-h/1500) + A exp(-h/1000) \tag{2.6}$$

where v is the rms wind speed in meters per second (m/sec), h is the altitude in meters (m) and A is a nominal value of $C_n^2(0)$ at the ground in $m^{-2/3}$. For FSO links near the ground, C_n^2 can be taken at an approximate of $1.7 \times 10^{-14} m^{-2/3}$ during daytime and $8.4 \times 10^{-15} m^{-2/3}$ at night. Overall, C_n^2 varies from $10^{-15} m^{-2/3}$ for strong turbulence to $10^{-17} m^{-2/3}$ for weak turbulence with $10^{-15} m^{-2/3}$ often defined as a typical average value [26].

CHAPTER 3

DERIVATION OF PAIRWISE ERROR PROBABILITY (PEP)

The pairwise (PEP) represents the probability of detecting the coded sequence $\hat{C} = (\hat{c}_1, \hat{c}_2, \ldots, \hat{c}_M)$ when $C = (c_1, c_2, \ldots, c_M)$ indeed was transmitted. We consider IM/DD links using OOK. Following [27], we assume that the noise can be modeled as additive white Gaussian noise (AWGN) with zero mean and variance $N_0/2$, independent of the on/off state of the received bit. Under the assumption of perfect channel state information (CSI), the conditional PEP with respect to fading coefficients is given as [27].

$$P(C, \hat{C}) = \int_0^\infty F(I)\, Q\left(\sqrt{\frac{\epsilon(C, \hat{C})}{2N_o}}\right) dI \tag{3.1}$$

where $\in (C, \hat{C})$ is the energy difference between two codewords and $Q(.)$ is the Gaussian-Q function. Since OOK is used, the receiver would only receive signal light subjected to fading during on-state transmission. Thus, we have

$$P(C, \hat{C}) = \int_0^\infty F(I) Q\left(\sqrt{\frac{E_s}{2N_0} \sum_{k \in \Omega} I_k^2}\right) dI \tag{3.2}$$

where Ω is the set of bit intervals' locations where C and $\hat{C}$ differ from each other and E_s is the total transmitted energy. Defining the signal-to-noise ratio as $\tau = E_s/N_0$ and using the alternative form for Gaussian-Q function, $Q = \left(\frac{1}{2\pi}\right)\int_0^{2\pi} exp\left(\frac{-x^2}{sin^2\theta}\right) d\theta$ we obtain

$$P(C,\hat{C}) = \frac{1}{\pi}\int\limits_{0}^{\frac{\pi}{2}} \left[\int\limits_{0}^{\infty} exp\left(-\frac{\tau}{4}\frac{I^2}{sin^2\theta}\right)f(I)dI\right]^{|\Omega|} d\theta \qquad (3.3)$$

$F(I)$ is the pdf for the gamma-gamma channel given by Eq. (2.3). Direct use Eq. (2.3) in Eq. (3.3), yields an expression which does not have a closed form solution unfortunately. To get around with this, we exploit the fact that the underlying distribution is a conditional gamma distribution with its mean μ following again a gamma distribution, and rewrite Eq. (3.3) as

$$P(C,\hat{C}) = \frac{1}{\pi}\int\limits_{0}^{\frac{\pi}{2}} \left\{E_\mu\left\{E_{\frac{I}{\mu}}\left[exp\left(-\frac{\tau}{4}\frac{I^2}{sin^2\theta}\right)\right]\right\}\right\}^{|\Omega|} d\theta \qquad (3.4)$$

The inner expectation in Eq. (3.4) for the gamma-gamma channel gives

$$E_{I/\mu}\left[exp\left(-\frac{\tau}{4}\frac{I^2}{sin^2\theta}\right)\right] = \frac{\beta^\beta}{\mu^\beta\Gamma(\beta)}\int\limits_{0}^{\infty} I^{\beta-1}exp\left(-\frac{\tau}{4}\frac{I^2}{sin^2\theta} - \frac{\beta I}{\mu}\right)dI \qquad (3.5)$$

Using the result from [28, Eq. 3.462.1, p. 382], i.e.

$$\int\limits_{0}^{\infty} z^{\nu-1}exp(-az^2 - bz)dz = (2a)^{-\nu/2}\Gamma(\nu)exp\left(\frac{b^2}{8a}\right)D_{-\nu}\left(\frac{b}{\sqrt{2a}}\right) \qquad (3.6)$$

where $Dp\,(\cdot)$ is the parabolic cylinder function, we obtain

$$E_{I/\mu}\left[exp\left(-\frac{\tau}{4}\frac{I^2}{sin^2\theta}\right)\right] = \frac{\beta^\beta}{\mu^\beta}\left(\frac{\tau}{2}\frac{1}{sin^2}\right)^{\frac{-\beta}{2}} exp\left(\frac{\beta^2 sin^2\theta}{2\mu^2\tau}\right)D_{-\beta}\left(\frac{\sqrt{2\beta}}{\mu\sqrt{\tau}}sin\theta\right) \quad (3.7)$$

Since the operation of expectation over μ required in Eq. (3.4) does not yield a closed form, we resort to the asymptotic expansion of the parabolic cylinder function given as [29, Eq.19.9, p.689].

15

$$D_{-\left(a+\frac{1}{2}\right)}(z) = \frac{\sqrt{\pi}}{\Gamma\left(\frac{3}{4} + \frac{a}{2}\right)} 2^{-\left(\frac{a}{2} + \frac{1}{4}\right)} exp\left(-\left(\sqrt{a} + \frac{1}{16}a^{-\frac{2}{3}}\right)z - O(z^2)\right) \quad (3.8)$$

where $O(z^n)$ represents the terms with power equal or higher than n. The above holds for $z^2 \ll a$ and this condition is easily satisfied in our case for high SNR values. Replacing the asymptotic expression in Eq. (3.7) and using the resulting expression in Eq. (3.4), we have Eq. (3.9).

$$P(C, \hat{C}) = \frac{1}{\pi} \int\limits_{0}^{\frac{\pi}{2}} \left[c1\tau^{-\frac{\beta}{2}}(sin\theta)^\beta \int\limits_{0}^{\infty} \mu^{\alpha - \beta - 1} exp\left(-\alpha\mu - c2\frac{\sqrt{2}sin\theta}{\sqrt{\tau}}\mu^{-1}\right. \right.$$

$$\left. \left. - O(\mu^{-2}) \right) d\mu \right]^{|\Omega|} d\theta \qquad (3.9)$$

where

$$c1 = \frac{\sqrt{\pi}\,\alpha^\alpha\beta^\beta}{\Gamma(\alpha)\Gamma\left(\dfrac{\beta + 1}{2}\right)}$$

$$c2 = \beta\left(\sqrt{\beta - \frac{1}{2}} + \frac{1}{16}\left(\beta - \frac{1}{2}\right)^{-\frac{3}{2}}\right) \qquad (3.10)$$

The inner integral can be solved with the help of [32, Eq. 3.471.9, p. 384]

$$\int\limits_{0}^{\infty} z^{\nu - 1} exp\left(-az - b\frac{1}{z}\right) dz = 2\left(\frac{b}{a}\right)^{\nu/2} K_\nu\left(2\sqrt{ab}\right) \qquad (3.11)$$

$a > 0, \ b > 0$. This yields the final form for PEP as Eq. (3.12), It should be emphasized that Eq. (3.12) is an approximation since the higher order components in the asymptotic expansion of the parabolic cylinder function are neglected.

$$P(C,\hat{C}) = \frac{1}{\pi} \int\limits_{0}^{\frac{\pi}{2}} \left[2^{\frac{\alpha-\beta+4}{4}} c1 \left(\frac{c2}{\alpha} \right)^{\frac{\alpha-\beta}{2}} \left(\frac{sin\theta}{\sqrt{\tau}} \right)^{\frac{\alpha+\beta}{2}} K_{\alpha-\beta} \left(2^{5/4} \sqrt{\frac{c2\alpha sin\theta}{\sqrt{\tau}}} \right) \right]^{|\Omega|} d\theta \qquad (3.12)$$

We plot in Fig. 2, the approximate derived PEP given by Eq. (3.12) for an error event of length 3, i.e. $/\Omega/=3$, using different links distances L1= 3000, L2= 4000, L3= 5000 which correspond to $x_1^2 = 1.031$, $x_2^2 = 1.747$, $x_3^2 = 2.63$, respectively. at wavelength $\lambda = 1550$ and $C_n^2 = 1.7 \times 10^{-14}$.
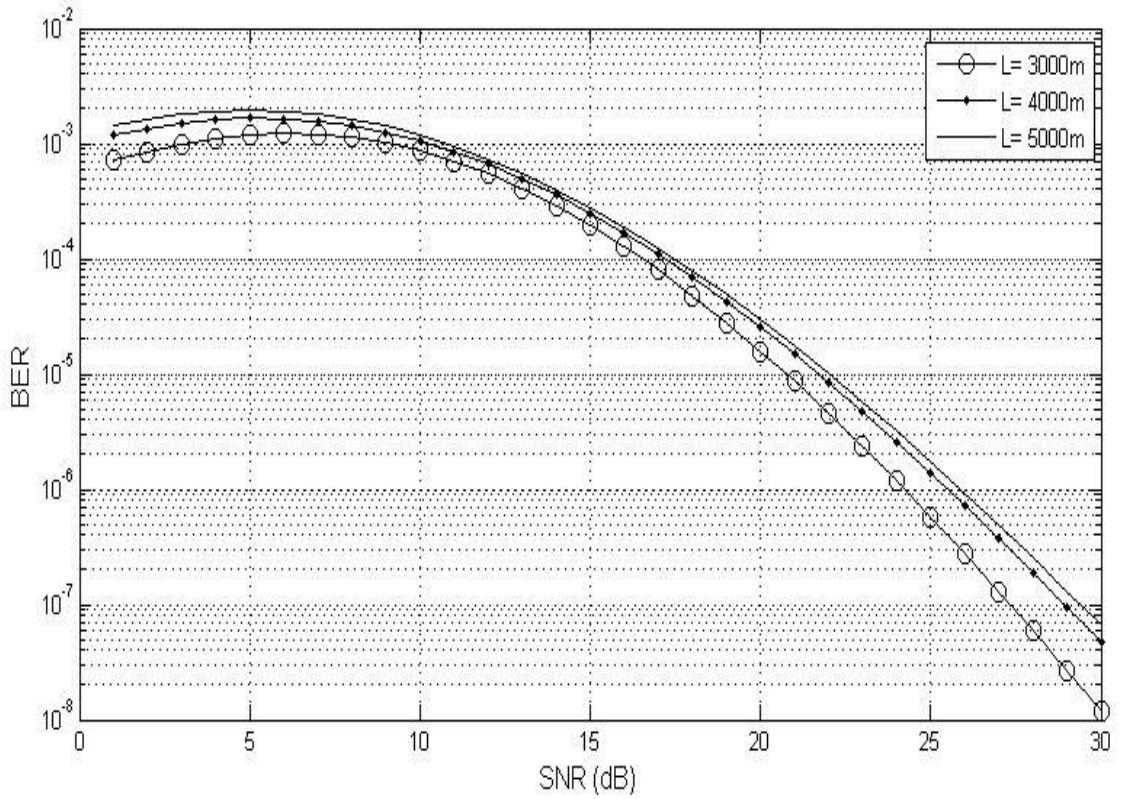

Figure 2: Comparison of the derived PEP in different link distances

CHAPTER 4

ERROR-PROBABILITY BOUNDS FOR CODING SCHEME

By using the approximate derived PEP codeword-error, we can compute the error probability for coding scheme. In this chapter, we consider block codes. We derive upper bounds on the bit-error probability of RS codes, BCH codes and Hamming codes. For block code (n, k) with a set of codewords $\{C_0, C_1, \ldots, C_{2^k-1}\}$, where C_0 denotes the all-zero codeword, the average bit-error probability upper bound is, [27].

$$E[P_b] \leq \frac{1}{k} \cdot \sum_{j=0}^{2^k-1} B_j E[P_e(C_j, C_0)] \tag{4.1}$$

where B_j is weight distribution of MDS codes of the information sequence corresponding to codeword C_j,

$$B_j = \binom{n}{j} \sum_{i=0}^{r-d_{min}} (-1)^i \binom{j}{i} \left(q^{j-d_{min}+1-i} - 1\right) \tag{4.2}$$

By using Eq. (4.2) in Eq. (4.1), we have final Eq. (4.3).

$$E[P_b] = \frac{1}{k} \cdot \sum_{j=1}^{2^k-1} \binom{n}{j} \sum_{i=0}^{r-d_{min}} (-1)^i \binom{j}{i} \left(q^{j-d_{min}+1-i} - 1\right) E[P_e(C_j, C_0)] \tag{4.3}$$

4.1. Review of Channel Coding Techniques

This section presents the three channel coding techniques that are considered in this

thesis, RS code, BCH code, and Hamming code. Since they are popular and traditional channel coding techniques then a brief analysis is presented.

4.1.1. Reed-Solomon Codes

Reed–Solomon (RS) code are non-binary cyclic error-correcting codes, RS codes are associated to the family of linear block codes and one of the most important class of MDS codes [31]. They are generally applied in data transmission systems that are submitted to destroy errors such as satellite communications. Furthermore, RS code differs from Hamming code in that it encodes groups of bits instead of one bit at a time.

Block length: $\qquad n = q - 1$

Information length: $\qquad k = n - r = n - 2t$

Minimum distance: $\qquad d_{min} = n - k + 1 = 2t + 1$

4.1.2. BCH Codes

The BCH codes are binary cyclic error-correcting codes. An essential property of BCH codes is that in code design there is specific control on the number of symbol errors that are correctable by the code, this is specific to the possibility of the designing of binary BCH codes that are able to correct multiple bit errors. The facilitation of the decoding of BCH codes is an advantage, since they are named by syndrome decoding which is an algebraic naming method. The use of low-power and small electronic hardware enable the simplicity of the design of the decoder for these codes [31]. BCH codes are applied in applications such as satellite communications making it applicable to random signal errors.

Block length: $\qquad n = 2^m - 1$

Information length: $\qquad k = 2^m - 1 - r = n - mt$

Minimum distance: $\qquad d_{min} = 2t + 1$

4.1.3. Hamming Codes

Hamming codes are still widely used in computing, telecommunication, and other applications including data compression. The hamming codes are associated as a family of linear block error-correcting codes, these are able to correct one-bit errors or detect a maximum of two-bit errors minus the detection of uncorrected errors [31]. When contrasting, the parity code and its simplicity is unable to correct errors and may only sense and odd number of bits in error. Hamming codes are known as flawless codes, since they are able to accomplish the highest rate possible for codes with their minimum distance and block length available.

Block length:	$n = 2^m - 1$
Information length:	$k = 2^m - 1 - m$
Minimum distance:	$d_{min} = 2t + 1 = 3$

CHAPTER 5

NUMERICAL RESULTS

In this chapter, we present the numerical results we obtained from the derived approximate error probability upper bounds given by Eq. (4.3) to evaluate the performance of some practical codes and compare the error probability with and without codes. Also we show results to compare the performances of the error probability under different codes and different code length (Hamming, Reed-Solomon and BCH) and turbulence schemes (weak, moderate and strong).

We study each code separately, starting from Hamming, Reed-Solomon to BCH codes. We consider FSO communication system operating over the gamma-gamma distribution at the wavelength $\lambda = 1550$ and $C_n^2 = 1.7 \times 10^{14}$, which is a typical value of refractive index structure constant for FSO links near the ground during daytime. Therefore we evaluate for each code (Hamming, Reed-Solomon and BCH) the BER performance over different link distances L1 = 3000m, L2 = 4000m, L3 = 5000m and different which correspond to $x_1^2 = 1.031$, $x_2^2 = 1.747$, $x_3^2 = 2.63$, respectively. After that we plot all codes (Hamming, Reed-Solomon, BCH) in one figure for each atmosphere turbulence (weak, moderate, strong).

5.1. BER Performance for Different Channel Coding

5.1.1. Hamming Code

First we study the Hamming (7, 4, 3) code as provided in Fig. 3. Here, we plot Upper bounds BER performance versus average SNR over different link distances of 3000 m, 4000 m and 5000 m. Comparing with the no-coding case, we notice that the BER performance with coding is improved for each link distance.

In Fig. 4, we plot the Upper bounds BER performance for different Hamming code length, namely (7, 4, 3) and (15, 11, 3) with $\lambda = 1550$, $x_2^2 = 1.747$ and $C_n^2 = 1.7 \times 10^{14}$ in order to compare with the no-coding case. It is seen that the BER performance is improved much better when the code length is increases to (15, 11, 3).
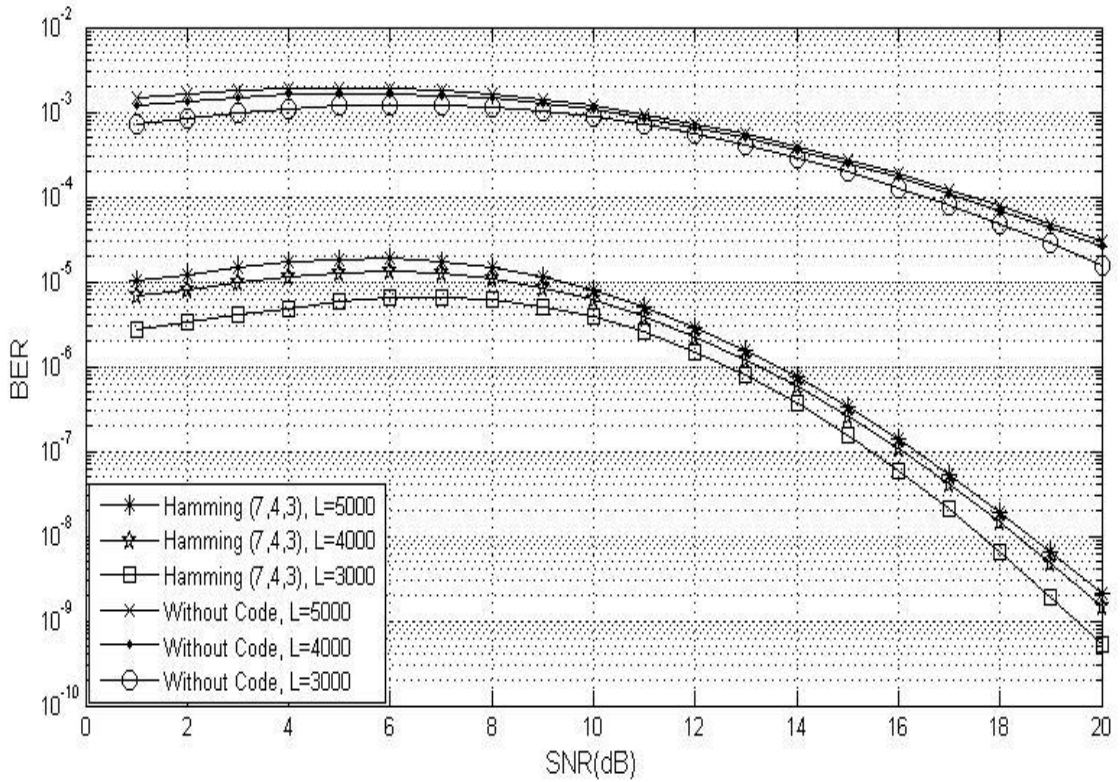

Figure 3: Upper bounds on BER performance for Hamming (7, 4, 3) code over different link distances compared without code case.
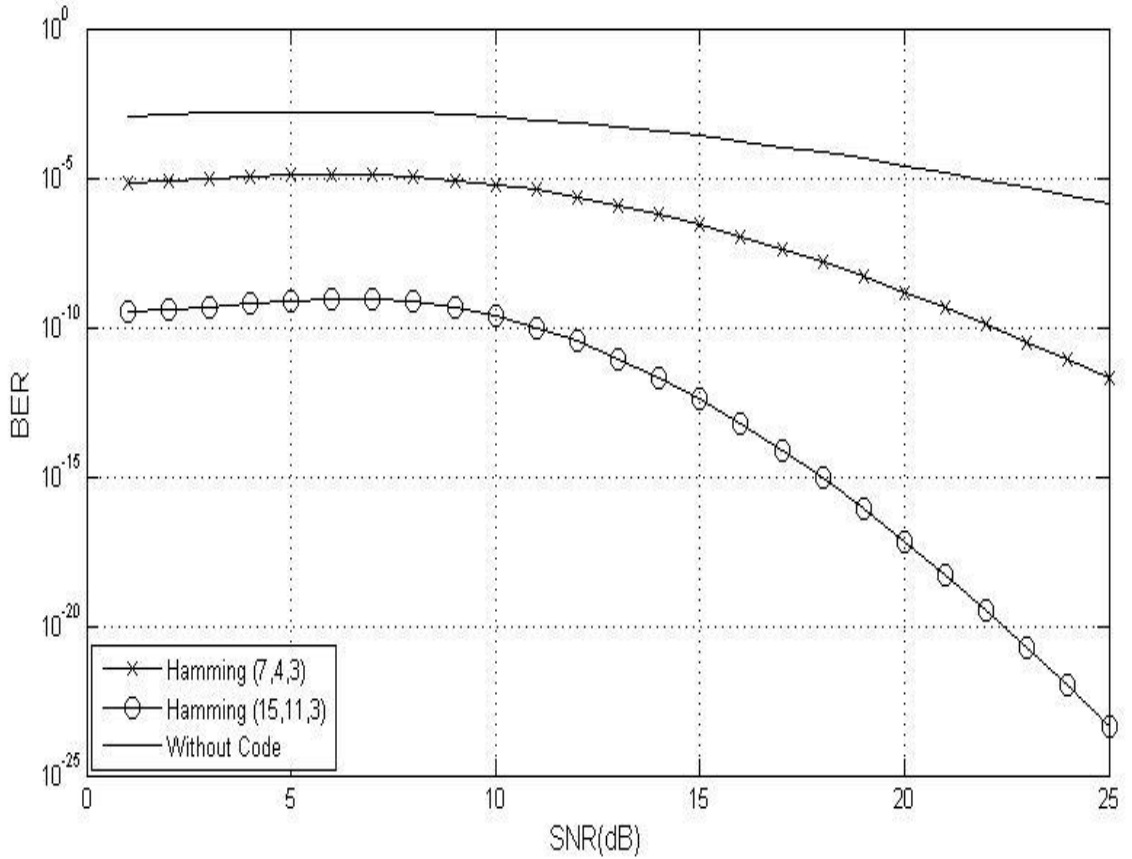
Figure 4: Upper bounds on BER performance for Hamming code in different code lengths (15, 11, 3) and (7, 4, 3) compared with no-coding case.

5.1.2. Reed-Solomon Code

In Fig. 5, we plot Upper bounds BER performance for Reed-Solomon (7, 5, 3) code as compared to the no-coding case over different link distances. We notice that the performance started getting better than the no-coding case at SNR >18dB for L=3000m, >19dB for L=4000m and >20dB for L=5000m. Also we plot the BER performance for different Reed-Solomon code length (15, 9, 7) and (7, 5, 3) and compared them with the no-coding case in Fig. 6. Here our aim is to show the effect of the increases in the code code length on the BER performance. It is seen that the BER performance increases much better in (15, 9, 7) as compared to the (7, 5, 3) case. In Fig. 6, $\lambda = 1550$, $x_2^2 = 1.747$ and $C_n^2 = 1.7 \times 10^{14}$.
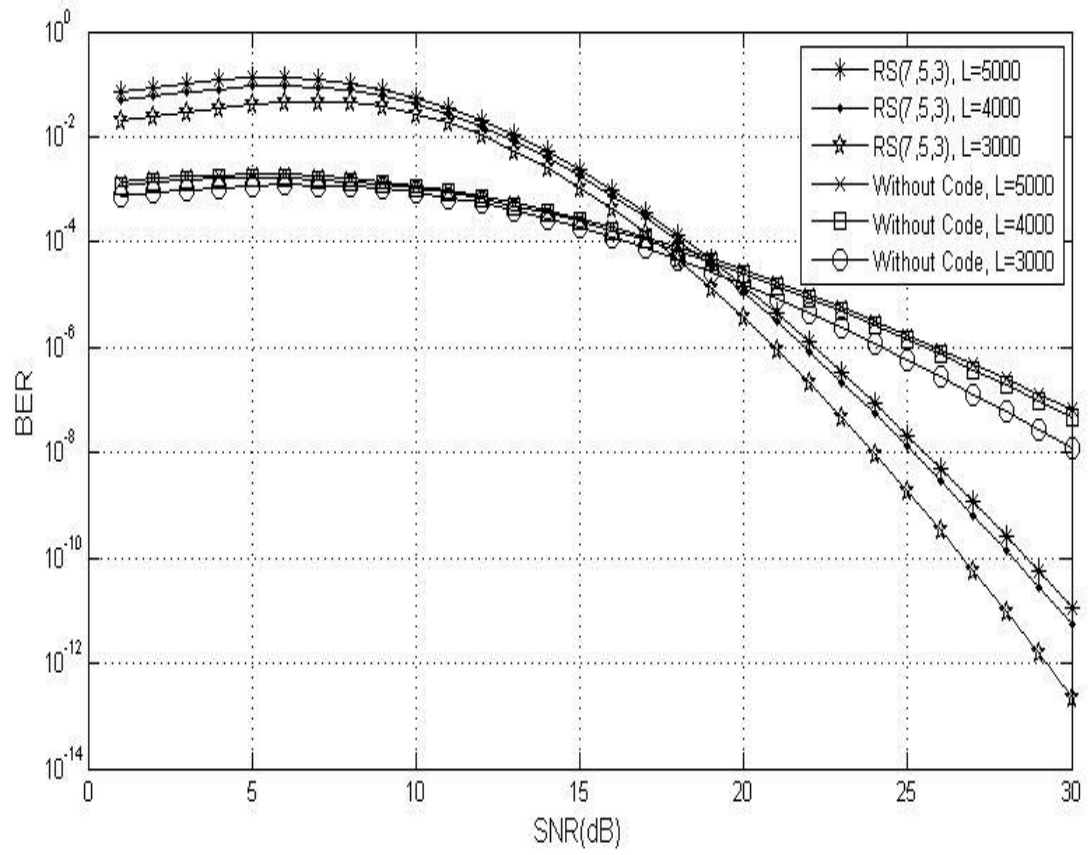
Figure 5: Upper bounds on BER performance for Reed-Solomon code (7, 5, 3) over different link distances compared with no-coding case.
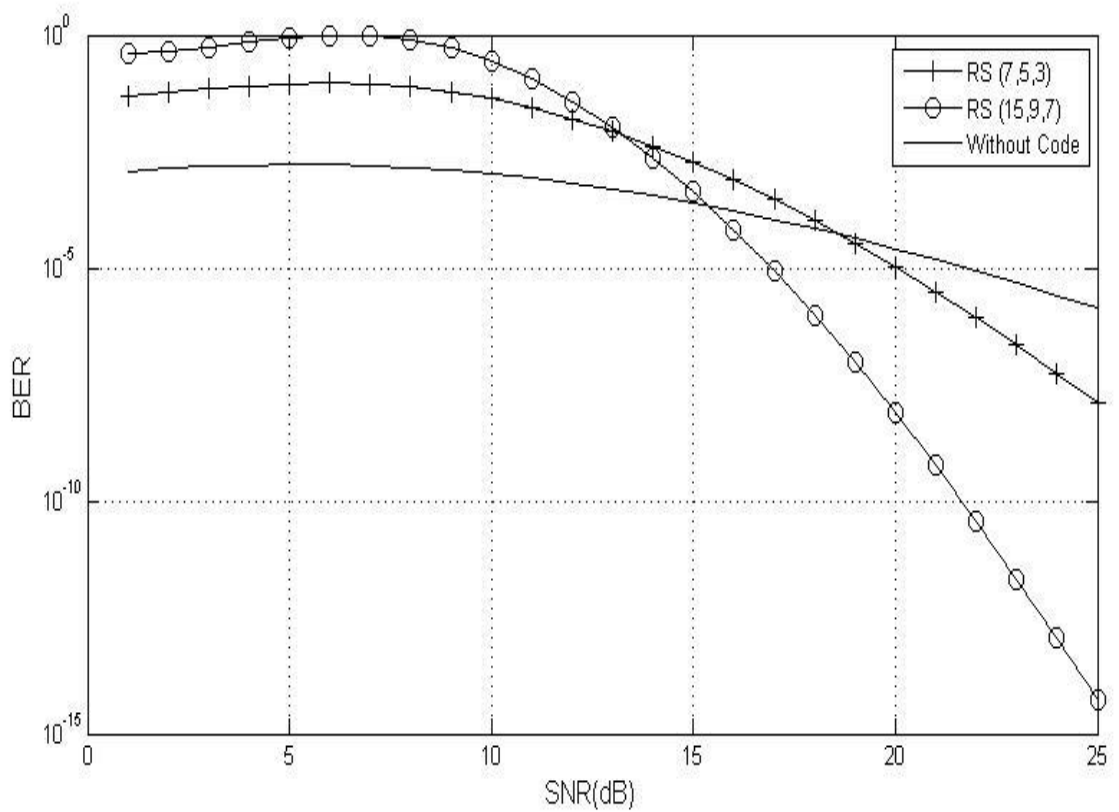
Figure 6: Upper bounds on BER performance for Reed-Solomon code (15, 9, 7) and (7, 5, 3) compared with no-coding case.

5.1.3. BCH Code

In Fig. 7. we plot the average BER performance for BCH (7, 4, 3) code over different link distances and compare these results with the no-coding case. Our purpose is to show the effect of BCH code on the BER performance. We find that the BER performance becomes much better as compared to the no-coding case. We show in Fig. 8, the effect of the increases in the code length on the BER performance. It is seen that the BER performance increases much better in BCH (15, 7, 5) as compared to (7, 4, 3). In Fig. 8, $\lambda = 1550$, $x_2^2 = 1.747$ and $C_n^2 = 1.7 \times 10^{14}$.
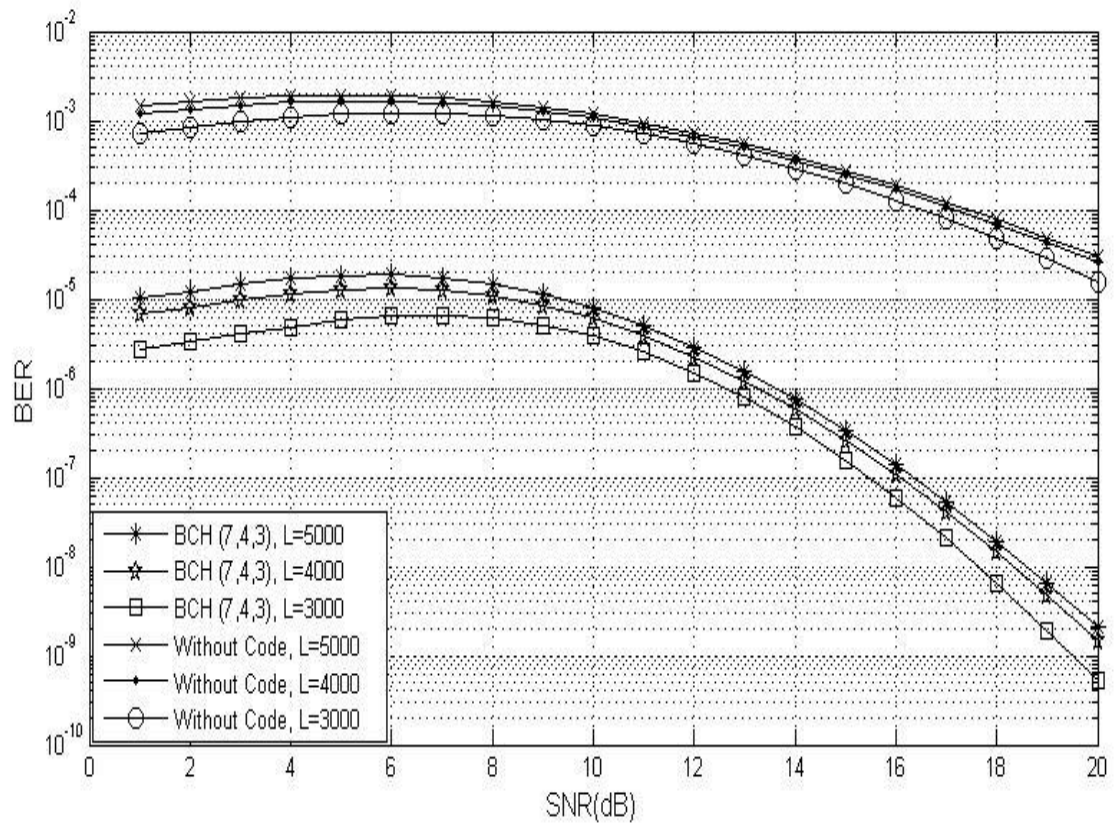
Figure 7: Upper bounds on BER performance for BCH code (7, 4, 3) over different link distances compared with no-coding case.
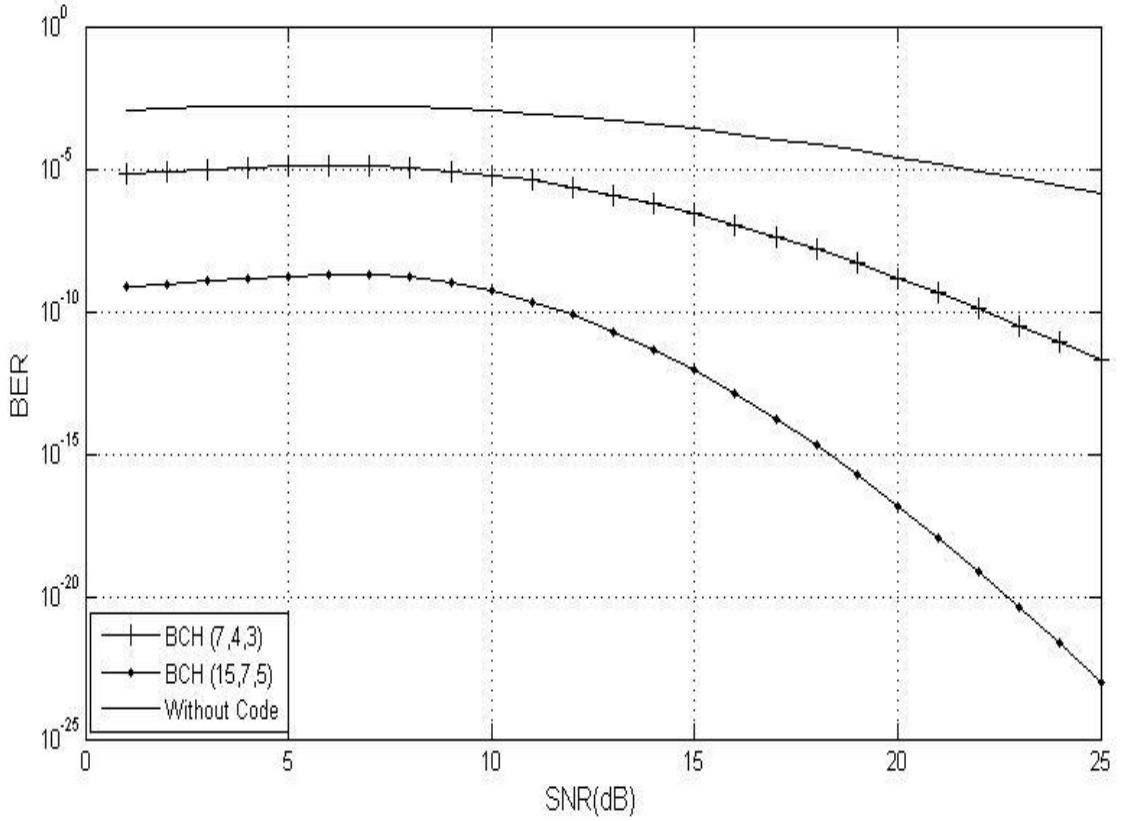
Figure 8: Upper bounds on BER performance for BCH (15, 7, 5) and (7, 4, 3) compared with no-coding case.

5.2. BER Performance for Different Turbulence Conditions

In section one of this chapter, we study the BER performance for each code separately in different link distances and different code values. In this section we plot the BER performance for all codes on different turbulence conditions to compare the performance of BER values for codes with different turbulence conditions.

We consider three typical cases of turbulence conditions, weak, moderate and strong. For this purpose, we set $x_2^2 = 0.5$, $C_n^2 = 8.6 \times 10^{-15}$, $\alpha = 4.62$, $\beta = 4.24$ for weak turbulence, $x_2^2 = 1.727, C_n^2 = 1.7 \times 10^{-14}$ $\alpha = 4$, $\beta = 2.56$ for moderate turbulence and $x_2^2 = 5.3$, $C_n^2 = 8.9 \times 10^{-14}$ $\alpha = 2.14$, $\beta = 1.21$ for strong turbulence. Also, we took the wavelength to be $\lambda = 1550$, the link distance as 3000 m and the code lengths for the Hamming (15, 11, 3), RS (15, 9, 7) and BCH (15, 7,5).

27

In Fig. 9, we plot upper bounds on BER performance for all codes on weak turbulence condition. The values chosen in Fig. 14 are $\lambda = 1550$, $x_2^2 = 0.5$, $C_n^2 = 8.6 \times 10^{-15}$, L= 3000 m, $\alpha = 4.62$, $\beta = 4.24$. Here, α and β are the effective number of small scale and large scale eddies of the scattering environment. It is seen that the coding channel increases the BER performance as compared to no-coding case, and the performance of the Hamming code is found to be better than the performances of the BCH and Reed-Solomon codes.

In Fig. 10, we plot upper bounds on BER performance for all the codes in moderate turbulence condition. Here, $\lambda = 1550$, $x_2^2 = 1.727$, $C_n^2 = 1.7 \times 10^{-14}$, L= 3000 m, $\alpha = 4$, $\beta = 2.56$ are used. It is seen that the coding channel increases the BER performance when compared to the no-coding case. It is also observed that the performance of the Hamming code is better than the BCH and the Reed-Solomon codes. The performance of BER in moderate turbulence is worse than the performance in weak turbulence.

In Fig. 11, we plot upper bounds on BER performance for all the codes in strong turbulence condition. Here, $\lambda = 1550$, $x_2^2 = 5.3$, $C_n^2 = 8.9 \times 10^{-14}$, L= 3000, $\alpha = 2.14$, $\beta = 1.21$ are used. Again, it is observed that the coding channel increases the BER performance as compared to the no-coding channel, and the performance of the Hamming code is found to be better than the BCH and the Reed-Solomon codes. The performance of BER is further decreased when compared to the BER performance in weak and moderate turbulence. To summarize, the performance of BER changes with the turbulence conditions, and whenever the turbulence strength becomes stronger, the BER performance become smaller.
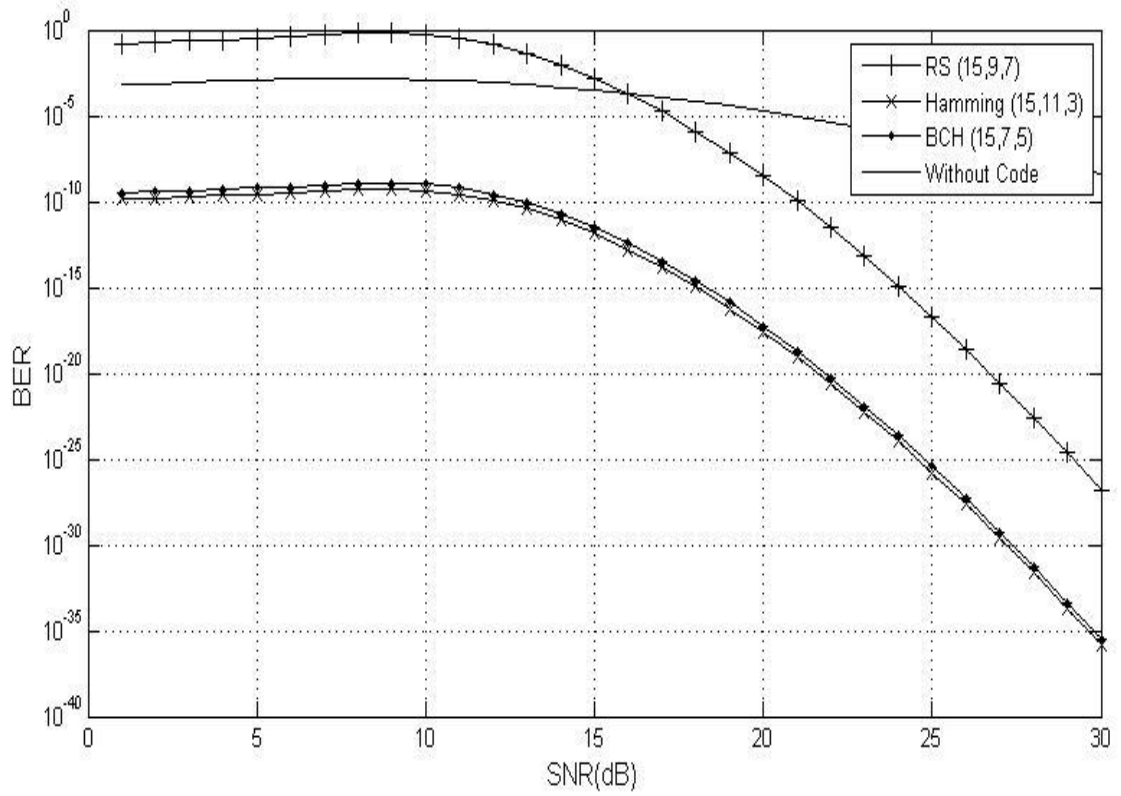
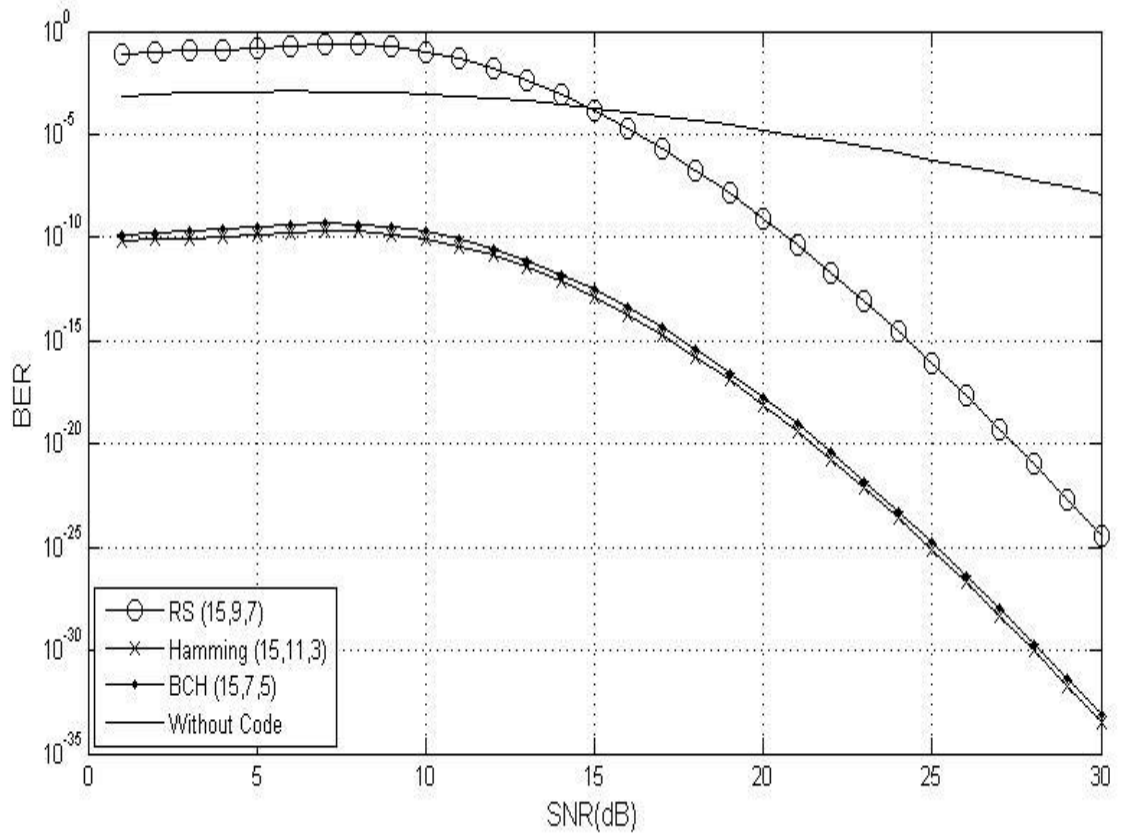**Figure 9:** Upper bounds on BER performance on weak turbulence condition.

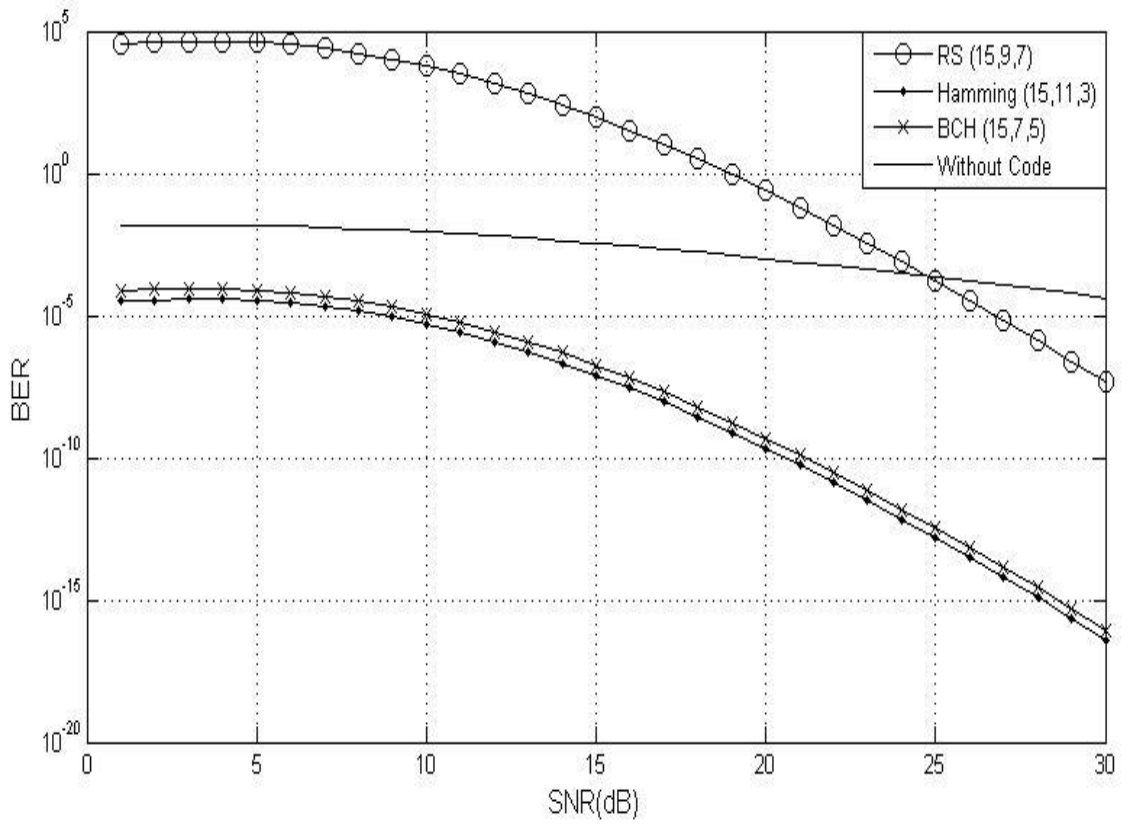**Figure 10:** Upper bounds on BER performance on moderate turbulence condition

Figure 11: Upper bounds on BER performance on strong turbulence condition.

CHAPTER 6

CONCLUSION AND FUTURE WORK

6.1. Conclusion

In this thesis, we have studied the coding channel performance on FSO communication systems operating over atmospheric turbulence channels. The turbulence is modeled with gamma-gamma pdf. Unlike the classically used log-normal pdf which is only accurate for modeling the weak turbulence, the gamma-gamma channel model works for a variety of turbulence conditions, weak, moderate and strong.

We first derived the pairwise (PEP) codeword-error probability for atmospheric turbulence channels with OOK. Then we derived the error performance bounds for various coding schemes through atmospheric turbulence channels, including the Reed-Solomon code, the Hamming code and the BCH code. We performed a comparative study of the performances of different channel coding techniques.

We plot the BER performance for each code separately in different link distances and different code lengths. We found that the BER performance gets much better when compared to no-coding case. Also we observe that the BER performance is improved when the code length is increased. Another conclusion is that the Hamming code shows better BER performance as compared to the BCH and the Reed-Solomon codes.

We then plot the BER performance for all the codes at different turbulence strengths, namely weak, moderate, strong regimes. The performances of BER when there is coding are compared with different turbulence conditions. The performance of BER is found to change with the turbulence conditions so that as the turbulence strength is increased, BER performance becomes less.

6.2. Future Work

In this thesis, we have investigated the channel coding performance on FSO communication system by using block codes (Reed-Solomon, BCH, and Hamming). Our future work is to study the channel coding error rate performances by using other kinds of codes and different techniques such as the multiple-input multiple-output (MIMO) systems in FSO and underwater optical communication systems. In addition, we intend to investigate the error rate performance over hyper RF-FSO links.

REFERENCES

1. **Zhijun Z., Rui L., Stephen D., and Michael C., (2010),** "*Reed-Solomon Coding for Free-Space Optical Communications Through Turbulent Atmosphere*", IEEEAC Paper 1273, Version 3, pp. 2.

2. **Bloom S., and Hartley W., (2002),** "*The Last-Mile Solution: Hybrid FSO Radio*", Air Fiber Inc, pp. 3–14.

3. **Heatley D., Wisely D., Neild I., and Cochrane P., (1998),** "*Optical Wireless: The Story so Far*", IEEE Communications Magazine, vol. 36, no. 12, pp. 72–74, 79–82.

4. **Juarez J., Dwivedi A., Hammons A., Jones S., Weerackody V., and Nichols R., (2006),** "*Free-Space Optical Communications for Next-Generation Military Networks*", IEEE Communications Magazine, vol. 44, no. 11, pp. 46–51.

5. **Hamkins J., (1999),** "*Performance of Binary Turbo-Coded 256- Ary Pulse-Position Modulation*", The Telecommunications and Mission Operations Progress Report pp. 42-138.

6. **Hemmati H., (2006),** Ed., "*Deep Space Optical Communications*", John Wiley & Sons, Inc., New Jersey, pp. 22–31.

7. **Andrews L., (2005),** "*Free-Space Laser Propagation: Atmospheric Effects*", Digest of the LEOS Summer Topical Meetings, vol. 19, no. 5, pp. 3.

8. **Gagliardi R. and Karp S., (1995), "***Optical Communications***",** Wiley, pp. 12.

9. **Andrews L. and Phillips R., (2005),** "*Laser Beam Propagation Through Random Media*", SPIE Press, Bellingham,Washington, USA, pp. 3.

10. **Andrews L., Phillips R., Sasiela R., and Parenti R., (2005),** "*Beam Wander Effects on the Scintillation İndex of a Focused Beam",* Proceedings of SPIE, vol. 5793, pp. 28– 37.

11. **Andrews L., Phillips R., and Hopen C., (2001), "***Laser Beam Scintillation with Applications***",** SPIE press, pp. 1–4.

12. **Tatarskii V., (1971),** "*The Effects of The Turbulent Atmosphere on Wave Propagation",* Jerusalem: Israel Program for ScientificTranslations, pp. 11.

13. **Fried D., (1967),** "*Aperture Averaging of Scintillation*", Journal of the Optical Society of America, vol. 57, pp. 169–172.

14. **Churnside J. H. and Hill R. J., (1987),** "*Probability Density of İrradiance Scintillations for Strong Path-İntegrated Refractiveturbulence",* Journal of the Optical Society of America , vol. 4, no. 4, pp. 727–733.

15. **Roggemann M. C. and Welsh B., (1996),** "*Imaging Through Turbulence",* CRC Press, New York, pp. 7.

16. **Dios F., Rubio J., Rodrguez A., and Comern A., (2004),** "*Scintillation And Beam-Wander Analysis in an Optical Ground Station-Satellite Uplink",* Applied Optics, vol. 43, no. 19, pp. 3866–3873.

17. **Anguita J., Neifeld M. A., and Vasic B., (2007),** "*Spatial Correlation and İrradiance Statistics in a Multiple-Beam Terrestrial Free-Space Optical Communication Link*", Applied Optics, vol. 46, no. 26, pp. 6561–6571.

18. **Zhu X. and Kahn J., (2002),** *"Free-Space Optical Communication Through Atmospheric Turbulence Channels"*, IEEE Transactionson Communications, vol. 50, no. 8, pp. 1293– 1300.

19. **Haas S., Shapiro J., and Tarokh V., (2002),** *"Space-Time Codes for Wireless Optical Communications",* EURASIP Journal on Applied Signal Processing, vol. 2002, no. 3, pp. 211–220.

20. **Weaver W. and Shannon C., (1959),** *"The Mathematical Theory of Communication",* University of Illinois Press Urbana, pp. 9.

21. **Blahut R., (2003) "***Algebraic Codes for Data Transmission"*, Cambridge University Press, pp. 6.

22. **Mceliece R., (1981),** *"Practical Codes for Photon Communication",* IEEE Transactions on Information Theory, vol. 27, no. 4, pp. 393–398.

23. **Andrews L. C., Phillips R. L., Hopen C. Y., and Al-Habash M. A., (1999),** *"Theory of Optical Scintillation",* Journal of Optical Society America , vol. 16, no. 6, pp. 1417-1429.

24. **Andrews L. C., Phillips R. L., and Hopen C. Y., (2000),** *"Aperture Averaging of Optical Scintillations : Power Fluctuations and the Temporal Spectrum",* Waves Random Media, vol. 10, pp. 53-70.

25. **Al-Habash A., Andrews L. C., and Phillips R. L., (2001),** *"Mathematical Model for the Irradiance Probability Density Function of a Laser Beam Propagating Through Turbulent Media",* Optical Engineering, vol. 40, no. 8, pp. 1554-1562.

26. **Goodman J. W., (1985), "***Statistical Optics"*, John Wiley &Sons, pp. 13–27.

27. **Zhu X. and Kahn J. M., (2003),** *"Performance Bounds for Coded Free-Space*

Optical Communications Through Atmospheric Turbulence Channels", IEEE Trans. Commun., vol. 51, no.8, pp. 1233-1239.

28. **Gradshteyn I. S. and Ryzhik I. M., (1994),** "*Table of Integrals, Series and Products"*, Academic Press, pp. 382.

29. **Abramowitz M. and Stegun I. S., (1977),** "*Handbook of Mathematical Functions with Formulas, Graphs and Mathematical Tables"*, Dover Publications, pp. 689.

30. **Uysal M., Jing L., and Meng Y., (2006),** *"Error Rate Performance Analysis of Coded Free-Space Optical Links Over Gamma-Gamma Atmospheric Turbulence Channels",* IEEE Transactions on Wireless Communications, vol. 5, no. 6. pp. 3.

31. **Moon K., (2005),** *"Error Correction Coding Mathematical Methods and Algorithms",* Published by John Wiley & Sons, Inc., Hoboken, New Jersey, pp. 42-87.

32. **Hranilovic S., (2005),** *"Wireless Optical Communication Systems*", Springer Science + Business Media, Inc. pp. 272–294.

33. **Arnon S., Barry R., Karagiannidis K., Schober R., Uysal M., (2012),** "*Advanced Optical Wireless Communication Systems",* Published in the United States of America by Cambridge University Press, pp. 36–59.

34. **Vetelino F. S., Young C., Andrews L. C., and Recolons J., (2007),** "*Aperture Averaging Effects on the Probability Density Function of Irradiance Fluctuations in Moderate-to-Strong Turbulence",* Applied Optics, pp. 2099–2108.

CURRICULUM VITAE

PERSONAL INFORMATION
Surname, Name: Abotabek, Ammar
Date and Place of Birth: 19 August 1988, Baghdad
Marital Status: Engaged
Phone: +90 531955 35 42
Email: ammarkais2000@yahoo.com

EDUCATION

Degree	Institution	Year of Graduation
M.Sc.	Çankaya University, Electronic and Communication Engineering, Ankara	2014
B.Sc.	University of Technology, Optoelectronics Engineering, Baghdad	2010
High School	Al-karkh High School, Baghdad	2006

WORK EXPERIENCE

Year	Place	Enrollment
01.2012-08.2012	**Dyako Group** CCTV and Security Solutions	*Sales Manager*
12.2010-01.2012	**Dyako Group** CCTV and Security Solutions	*CCTV Engineer*

FOREIGN LANGUAGES
Native Arabic, Advanced English, Average Turkish

HOBBIES
Reading, Writing, Traveling, Swimming